Journal of Photochemistry & Photobiology, A: Chemistry 426 (2022) 113759

Contents lists available at ScienceDirect

Journal of Photochemistry & Photobiology, A: Chemistry

journal homepage: www.elsevier.com/locate/jphotochem

Protonation, exciplex, and evidence of aggregate formation in *meso*-tetra (4-pyridyl) porphyrin triggered by excited-state absorption

J.M.S. Lopes [a,*], A.E.H. Machado [b], A.A. Batista [c], P.T. Araujo [d,*], N.M. Barbosa Neto [a,*]

[a] Institute of Natural Sciences, Graduate Program in Physics, Federal University of Pará, Belém, PA, Brazil
[b] Department of Chemistry, Federal University of Catalão, Catalão, GO, Brazil
[c] Department of Chemistry, Federal University of São Carlos, São Carlos, SP, Brazil
[d] Department of Physics and Astronomy, University of Alabama, Tuscaloosa, Alabama, United States

ARTICLE INFO

Keywords:
Excited-state absorption
Porphyrin protonation
Chloroform decomposition
Fluorescence quenching
Exciplex
Porphyrin aggregate

ABSTRACT

Excited-state absorption (ESA) portraits a new pathway to controllably generate hexaprotonated (H_8TPyP^{6+}) porphyrins followed by the formation of a new species (possibly porphyrin aggregate) departing from pristine *meso*-(4-pyridyl) porphyrins (H_2TPyP) dissolved in chloroform ($CHCl_3$). Steady-state absorption and photoluminescence (PL) spectroscopies provide solid signatures for each step of the process. The photo-protonation mechanism involves $CHCl_3$ decomposition driven by oxi-reduction reactions catalyzed by the H_2TPyP itself. Time-resolved PL shows that the dispersion of chloride ions (Cl^-) in the solution, which are remnant from the photo-triggered $CHCl_3$ decomposition, leads to the quenching of both H_2TPyP and H_8TPyP^{6+} emission lifetimes. Stern-Volmer analysis suggests that the H_8TPyP^{6+}'s excited-state interactions with Cl^- are non-emissive exciplex. Our findings open opportunities for the development of novel and controllable molecular processing strategies.

1. Introduction

Molecular excitation mechanisms, i.e., the pathways and rules obeyed during light-matter interaction, are closely associated with how efficiently photochemical reactions (PR) occur. Several PR are driven by the so-called one-photon absorption process (OPA) (e.g. photosynthesis [1] and vision's mechanisms [2,3]) and more recently pulsed lasers have been adopted as reliable sources to favor PR via alternative excitation pathways [4–6]. This is possible because the photon density delivered by pulsed lasers can promote non-linear light absorption processes such as non-resonant two-photon absorption (2PA) or excited-state absorption (ESA) [7,8]. According to Laport's rule [9], in ESA, the reactants' excited-state orbitals display distinct parities with relation to the parities associated with OPA, and such distinction could, in principle, favor different reaction mechanisms. Regardless the non-linear process, they paved ways for remarkable advances in, for example, photodynamic therapy [10,11], materials processing [12–14], and optical microscopy [15,16]. More recently, Barbosa-Neto and co-workers [12] have unveiled the routes to use ESA for controllable photo-aggregation of P3HT and the formation of highly stable polaron states in such aggregates. The work also shows that ESA presents higher aggregation efficiencies when compared with the standard OPA-induced aggregation using UV light source [12,17].

Ultra-Violet light has also been vastly utilized to trigger the decomposition of chlorinated solvents such as chloroform ($CHCl_3$). In one hand, when only solvents are involved, the photo-decomposition is directly driven by UVC photolysis [18,19]. On the other hand, when solutions are involved, the solute might work as mediators that catalyze such decomposition processes that are now driven by UVB and UVA [20–25]. Many structures, such as hexachloroosmate(IV) [20], hexachlororhodate(III) [21], Titanium dioxide [24], free-base porphyrins [25], and chlorochromate ion [26] have been employed as mediators. These mediators might also display absorption bands in the visible and near-IR spectral range, justifying the exploration of other mechanisms (e.g., ESA) to replace UV irradiation. Many applications require an understanding of solvent decomposition. Such understanding requires precise, reproducible, and controllable routes that allow for mapping the several steps involved in the process. In this context, the replacement of UV irradiation is highly desirable since it triggers unwanted degradation mechanisms whose origins are often obscure. Moreover, in solution, UV light is harmful not only for the solvent but also for organic mediators adding even more sources of spurious mechanisms. Therefore, ESA becomes an excellent alternative to the UV-light because it operates in the visible range, which fulfills all the energetic requirements without

* Corresponding author.
E-mail addresses: lopesjefferson01@yahoo.com.br (J.M.S. Lopes), paulo.t.araujo@ua.edu (P.T. Araujo), barbosaneto@ufpa.br (N.M. Barbosa Neto).

https://doi.org/10.1016/j.jphotochem.2021.113759
Received 17 August 2021; Received in revised form 19 November 2021; Accepted 28 December 2021
Available online 4 January 2022

compromising the mediator's integrity.

Porphyrins are exceptional candidates for mediators, displaying (1) a broad absorption window ranging from UV to near-IR [27,28]; (2) relaxation pathways including intersystem crossing and fluorescence [29]; and (3) effective ways to self-probe PR kinetics and fundamental processes associated with the interaction between remnant decomposition products and the porphyrins themselves (e.g., PL quenching mechanisms), by mapping their spectroscopic signatures [25,30]. These spectroscopic signatures come from the porphyrin macro ring [28], whose center comprises four nitrogen atoms linked to two hydrogen atoms (one 2^+ ion) in the case of free base (-metallo) porphyrins. Moreover, porphyrins are great ESA-driven absorbers' candidates, opening the possibility to their use as selection-rule controlled PR mediators. It is important to mention that, when porphyrins are irradiated with nanosecond pulses ESA prevails on 2PA since porphyrins present low 2PA absorption cross-sections [4,31,32]. Although nanosecond pulses do not have enough peak intensity to create a 2PA in free-base tetrapyridyl porphyrin (H_2TPyP) capable to compete with absorption at resonant conditions, they have enough fluence to transfer the ground state population to the first singlet excited-state and consequently to promote ESA.

Here we show how ESA applied to H_2TPyP [29] opens other excitation pathways that facilitate controllable $CHCl_3$ oxi-reduction decomposition [25]. Chloroform decomposition releases hydrochloric acid (HCl) in the solution, which is promptly detected through the protonation of the H_2TPyP's macro-ring. We also show that ESA can establish an ideal environment to allow for understanding the elusive PL quenching of both H_2TPyP and its protonated counterpart. The analysis of the Stern-Volmer (SV) plots indicates that the quenching is likely caused by the formation of non-emissive exciplex involving porphyrins and remnant Cl^- ions. We also demonstrate that, after achieving a critical concentration of protonated porphyrins, new photo species are controllably promoted by ESA (probably photo aggregated species).

2. Materials and methods

2.1. Pulsed and continuous (CW) laser sources

A frequency-doubled Q-switched Nd-YAG laser (operating at 20 Hz), from Quantel (Q-smart 100) with 6 ns FWHM pulse width ($\lambda_{exc} = 532$ nm and 1064 nm) was adopted as the pulsed-irradiation source. Each pulse presents a nominal fluence value of ~836 mJ/cm^2. The irradiation of solutions with continuous light was performed using blue (475 nm) and green (532 nm) CW lasers, from Laserline.

2.2. Sample preparation and spectroscopic measurements

Meso-tetra-substituted free-base (4-pyridyl) (H_2TPyP) porphyrin was synthesized according to procedures described in the literature [33]. During the spectroscopic measurements and irradiation processes, H_2TPyP is dissolved in three distinct solvents: chloroform ($CHCl_3$) stabilized with amylene, dimethyl sulfoxide (DMSO), and tetrahydrofuran (THF). All solvents were purchased from NEON and were used as received. The concentrations were all set to values $\leq$5 μM to avoid spontaneous aggregate formation.

Absorption spectra were acquired with a JASCO V-670 spectrophotometer. Steady-state fluorescence spectra were acquired using a setup composed of a Xenon lamp from ACTON; a monochromator model 300i by ACTON and a portable Ocean Optics spectrophotometer. The excitation wavelengths were selected by a monochromator and the fluorescence was detected in a 90° degree geometry (taking the direction of the excitation beam as reference). Time-resolved fluorescence experiments were performed using a *Time-Correlated Single Photon Counting* (TCSPC) Delta-Flex system from Horiba, equipped with a pulsed LED as the excitation source (352 nm at a repetition rate of 8.0 MHZ) and presenting a time/channel relation of 27 ps per channel. The decay curves were collected at 650 nm, which is approximately the most intense fluorescence peak observed for H_2TPyP. For all spectroscopic measurements and irradiation experiments, the samples are placed in 1.0 cm path length quartz cuvettes with four polished windows.

2.3. Quantum chemical calculations

All calculations are performed with Gaussian and the structures are obtained employing the Gaussview program [34]. The molecular structures are optimized via the M06 functional. The calculations of the orbitals and free energies are performed in a solvation environment, which is simulated in chloroform by the continuum dielectric model (IEFPCM). All calculations are performed considering the 60 first singlet excited-states of the molecules.

3. Results and discussion

3.1. Photo-induced modifications in absorption and photoluminescence features of H_2TPyP

Irradiation of H_2TPyP dissolved in $CHCl_3$ using a nanosecond pulsed laser (6.0 ns, 532 nm) induces significant changes in the original absorption spectrum, as shown in Fig. 1. From 0 to 400 J/cm^2 the intensity of the B-band originally centered at 417 nm (Fig. 1a) progressively decreases at the expense of creating an unforeseen band (from now on X-band) originally centered at 444 nm. The characteristic sigmoidal behavior (see inset in Fig. 1a), observed for the intensities of both $B(0,0)$ and the X-band with increasing fluence, together with the isosbestic point around 425 nm, suggests that this novel band is associated with a novel species originated from H_2TPyP [35,36]. Regarding the Q-bands (Fig. 1b), although novel bands are not observed, there are clear modifications in the peaks' relative intensities, which are also accompanied by an overall redshift. Fig. S1 in the supporting information (SI) shows a power-law correlation with the exponent approximately equal to 1 (~1.16 to $Q_x(0,0)$ band at 648 nm and ~0.91 to $Q_y(0,1)$ band at 513 nm) for the intensity evolution of the X-band with the $Q_x(0,0)$ and $Q_y(0,1)$ bands with changing fluence, which endorses that the features arise from the same photoproduct. It is important to note that pulsed radiation takes H_2TPyP out of its optical linear regime [29]. Therefore, we hypothesize that pulsed radiation is key to generating the new species. As shown in Fig. S2 in SI, when the solution is excited with continuous radiation (475 nm and 532 nm) under several distinct fluences (up to 60 times greater than those for pulsed radiation), no changes, whatsoever, are observed in the original spectra. Moreover, no spectral change is observed when the solution is excited with pulsed radiation at 1064 nm, corroborating the hypothesis that ESA is the process responsible to trigger the PR. We also hypothesize that having $CHCl_3$ as the solvent highly favors the development of new species. This hypothesis is verified by performing the same experiment in solutions of H_2TPyP dissolved in tetrahydrofuran (THF) and dimethyl sulfoxide (DMSO). Fig. S3 in SI shows, once again, that no changes in the original spectra are observed at all.

The spectral evolution with fluence leads us to understand that the photoproduct obtained here is a form of protonated porphyrin. Indeed, similar results have been observed in the literature where both acid solutions [30,36–43] and light irradiation [25,44,45] are used as the protonation agents. The literature discusses that protonation depends closely on the porphyrin structure and that such protonation usually takes one of the following routes, each of them with very specific spectral signatures: (1) only the porphyrin central ring undergoes protonation. In this case, a new and well-resolved band, which is often tens of nanometers redshifted from the original B-band, appears at the expense of decreasing the B-band intensity [42]; (2) only the porphyrin outlying groups undergo protonation. In this case, the B-band is slightly redshifted with relation to the original B-band position (usually units of

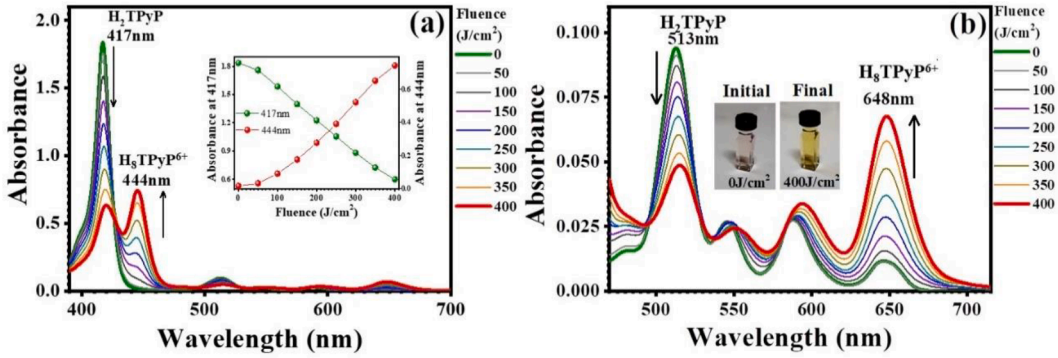

Fig. 1. Evolution of H_2TPyP absorption spectra as a function of pulsed laser fluence (0–400 J/cm^2) evaluated at (a) B and (b) Q bands. The inset in figure (a) compares the decreasing and increasing of the main B band constituting the H_2TPyP spectrum and its protonated counterpart H_8TPyP^{6+} cation (X-band), respectively. The inset in figure (b) shows the color variation of the solution after pulsed irradiation. The porphyrins are dissolved in $CHCl_3$.

nanometers) [46]; or (3) first, the outlying groups undergo protonation followed by the protonation of the central ring. In this case, both spectral modifications discussed in (1) and (2) occur in sequence [46]. In particular, Fang et al. describe the routes (1) to (3) very well for *meso*-pyridyl porphyrins [46]. Our method introduces a new route in which routes (1) and (2) occur simultaneously instead of in sequence. In this scenario, both outlying groups and the central rings undergo simultaneous protonation. Such an elusive route possesses clear spectral signatures (see Fig. 1a and Fig. S4 in SI) and shows that the final product obtained via ESA is the hexaprotonated porphyrin H_8TPyP^{6+}. In fact, theoretical calculations show that the $6H^+$ protonation of H_2TPyP in $CHCl_3$ presents $\Delta G = -313.32$ kJ/mol (free Gibbs' energy) and $\Delta H = -313.28$ kJ/mol (enthalpy) indicating that the protonation is thermodynamically favorable.

Additionally, we inspected the spectra under 0 J/cm^2 and 400 J/cm^2 applying both, deconvolution and spectral derivative methods, which the authors have thoroughly discussed elsewhere (see Figs. S5 in SI) [27,47]. The B-band from the original solution (0 J/cm^2), Fig. S5a, comprises two transitions: the electronic $B(0,0)$ and the vibronic $B(0,1)$ [27]. The solutions under 400 J/cm^2 (Fig. S5b), however, seem to comprise four sub-bands: 2 electronic ($B(0,0)$-like) and 2 vibronic ($B(0,1)$-like). The $B(0,0)$ and $B(0,1)$ bands from H_8TPyP^{6+} are in good agreement with the literature [40,41].

Steady-state photoluminescence (PL) and emission decay signatures from both H_2TPyP and protonated porphyrins are well documented in the literature [30,36–43] and corroborate the hypothesis and observations above. As seen in Fig. 2a, the $Q(0,0)$-band red-shift followed by a decrease of the intensity ratio $\frac{Q(0,1)}{Q(0,0)}$ reveals that the modifications in H_2TPyP PL emissions with increasing fluence are fully connected with the raise of PL emissions from protonated porphyrins [30,36–43]. Fig. 2b shows that the PL decay curves evolve from a mono-exponential curve associated solely with H_2TPyP ($\tau_1 = 7.26$ ns at 0 J/cm^2) to a bi-exponential associated with both H_2TPyP ($\tau_1 = 7.13$ ns) and H_8TPyP^{6+} ($\tau_2 = 1.28$ ns) at 100 J/cm^2. It is also noticeable (see Table 1) that both τ_1 and τ_2 steadily decrease with increasing fluence due to a quenching mechanism that is thoroughly explained later in the text (Section 3.3) [27,30,36].

3.2. Porphyrin assisted chloroform decomposition

As discussed above, the photo-induced protonation of H_2TPyP requires excitation and solvent optimal conditions. It is well established

Table 1
Excited-state decay parameters evolution of solutions containing only H_2TPyP to solutions containing both H_2TPyP and H_8TPyP^{6+} as a function of pulsed laser fluence (0–400 J/cm^2). The values in parentheses in the emission lifetime columns (τ_1 and τ_2) represent the percentage contribution of each exponential adopted in the fitting. $\chi 2$ estimates the fitting precision.

Fluence (J/cm^2)	τ_1 (ns)	τ_2 (ns)	$\chi 2$
0	7.26 (100%)	–	1.03
50	7.20 (100%)	–	1.04
100	7.13 (98%)	1.28 (2%)	1.04
150	7.01 (96%)	0.96 (4%)	1.00
200	6.92 (92%)	0.81 (6%)	1.07
250	6.85 (90%)	0.78 (10%)	1.05
300	6.26 (86%)	0.73 (14%)	1.07
350	6.68 (81%)	0.70 (19%)	1.09
400	6.71 (79%)	0.68 (28%)	1.08

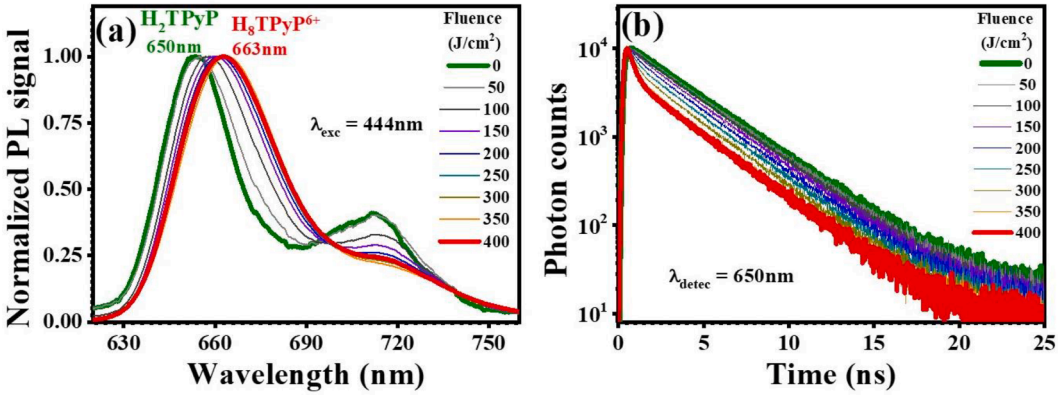

Fig. 2. (a) Normalized PL spectra ($\lambda_{exc} = 444$ nm) and (b) emission decay curves as a function of pulsed laser fluence. The excited-state decays were excited at 352 nm and probed at 650 nm. The porphyrins are dissolved in $CHCl_3$.

that, differently from CW lasers, nanosecond pulsed lasers easily induce ESA in porphyrins [8,48–56]. Therefore, PR might differ from each other according to the laser source used and the system under investigation [12,17]. In one hand, upon 532 nm (2.33 eV) and 475 nm (2.61 eV) CW excitations, our results do not show any evidence of PR. On the other hand, PR is readily observed under ESA, which is a sequential two-photon process [7]. In our experiments, ESA excites the molecule at 4.66 eV, which endorses the molecular energy threshold required to trigger the said PR (between 2.61 eV and 4.66 eV).

Munõz and co-workers have investigated tetraphenyl free base porphyrin (H_2TPP), which present electronic and vibronic properties similar to those of H_2TPyP [25,27,57]. They report a self-consistent mechanism in which 289 nm (4.29 eV) CW irradiation triggers a photooxidative excited-state in H_2TPP dissolved in $CHCl_3$. This photo-oxidative excited-state leads to the catalytic reduction of $CHCl_3$, which also releases HCl in the solution. The presence of HCl closes the cycle, by causing the formation of core-di protonated H_4TPP^{2+} porphyrin species. In other words, H_2TPP acts not only as a catalyst but also as an HCl sensor (other chromophores have also been used for the same purpose [20–26,58]). In our case, the ESA energy excitation is slightly higher than the excitation energy used by Munõz et al., [25] suggesting that H_2TPyP is protonated after achieving a photooxidative excited-state as well. This justifies the absence of PR in THF and DMSO solutions. Moreover, our results demonstrate that the protonation mechanism does not depend on the absorption selection rules since it is achievable with both ESA ($\lambda_{exc} = 532$ nm) and CW($\lambda_{exc} = 289$ nm) [25].

Other recent reports [44,45] have also shown that porphyrin's photo-induced protonation in chlorinated solvents occurs after solvent decomposition and HCl release. Those works, however, claim that solvent decomposition occurs due to porphyrin-independent photolysis driven by 2PA processes. In our context, this claim is inconsistent since, on several occasions [4–7,59], nanosecond pulsed lasers fail to promote 2PA in porphyrin at resonant conditions. Direct excited-state absorption is also excluded because $CHCl_3$ is transparent to visible radiation (see Section S2 in SI for a thorough discussion).

3.3. Excited-state lifetimes of H_2TPyP and H_8TPyP^{6+} and quenching mechanisms.

Our results show that the excited-state lifetimes from both H_2TPyP (τ_1) and H_8TPyP^{6+} (τ_2) decrease relative to their initial values ($\tau_{1(0)}$ and $\tau_{2(0)}$, respectively) with increasing radiation dosage (see Table 1) indicating a quenching process. In our case, due to the Q-bands' absorption-emission overlap between H_2TPyP and H_8TPyP^{6+}, the quenching mechanism could be explained via the radiative energy transfer process (see Fig. S6 in SI). We rule this possibility out because the absorbance involved here ($\ll 0.1$) is not large enough to trigger the aforementioned process; if such a process was taking place, it would manifest as an emission lifetime increase for at least one of the emitters [60–63] (see Section S3 in the SI).

We hypothesize, therefore, that the relative amplitude and emission lifetime decrease occur because the protonation mechanism we observe involves mass conservation among species. In other words, the decrease of the H_2TPyP's concentration with increasing radiation dosage is proportional to the increase of both H_8TPyP^{6+} and Cl^- concentrations (see Fig. S7 in SI). Our hypothesis is aligned with the fact that concentration-driven modifications in excited-state dynamics are often connected with intermolecular interactions leading to bimolecular quenching processes commonly understood in terms of so-called Stern-Volmer (SV) plots [60–62]. In our case, we assume that such intermolecular interactions are largely mediated by the Cl^- ions and that any other intermediate product arising from $CHCl_3$ decomposition is unstable [20–26,58].

Fig. 3 shows the SV plots for H_2TPyP $\left(\frac{\tau_{1(0)}}{\tau_1}\right)$ and H_8TPyP^{6+} $\left(\frac{\tau_{2(0)}}{\tau_2}\right)$ lifetime ratios as a function of both delivered fluence and Cl^- concentration (for details about the Cl^- concentration calculation, see Fig. S7 in the SI and related discussion). Two different quenching behaviors are observed: $\frac{\tau_{1(0)}}{\tau_1}$ quenches linearly (expected in dynamic quenching processes) while $\frac{\tau_{2(0)}}{\tau_2}$ follows a non-linear quenching. These distinct quenching behaviors are readily understood under the following assumptions: (i) H_2TPyP is not a quencher for H_8TPyP^{6+} since, as discussed earlier in the text, its concentration is decreasing (see Fig. 1); and (ii) both H_8TPyP^{6+} and Cl^- are quenchers for H_2TPyP, which is supported by the literature [64–73]. In fact, the higher concentration of Cl^- relative to that for H_8TPyP^{6+} favors its effectiveness as a quencher.

The deviation of SV plots from the linear behavior shown in Fig. 3a is commonly associated with exciplex (H_8TPyP^{6+}/Cl^- pairs) formation, which in our solutions is highly favored by strong electrostatic interactions between H_8TPyP^{6+} and Cl^- [60,61,74,75]. Note that Cl^-/H_2TPyP pairs experience weak electrostatic interactions, which highly disfavors exciplex formation. This understanding allows us to quantitatively evaluate the quenching effectiveness in our system. For such, the $\frac{\tau_{1(0)}}{\tau_1}$ curve in Fig. 3a is adjusted using the standard SV equation:

$$\frac{\tau_{1(0)}}{\tau_1} = 1 + K_{SV}[Cl^-], \quad (1)$$

where $K_{SV} \cong 0.488 \times 10^4\ M^{-1}$ is the quenching constant and $[Cl^-]$ is the chloride ion concentration.

The $\frac{\tau_{2(0)}}{\tau_2}$ curve is adjusted following Grosso and co-workers [74] and Kuzimin and co-workers [75]. Their work also investigates non-emissive exciplexes and, to adjust their non-linear curve, they modify Eq. (1) to include the exciplex contribution to the quenching mechanism. The new Equation is:

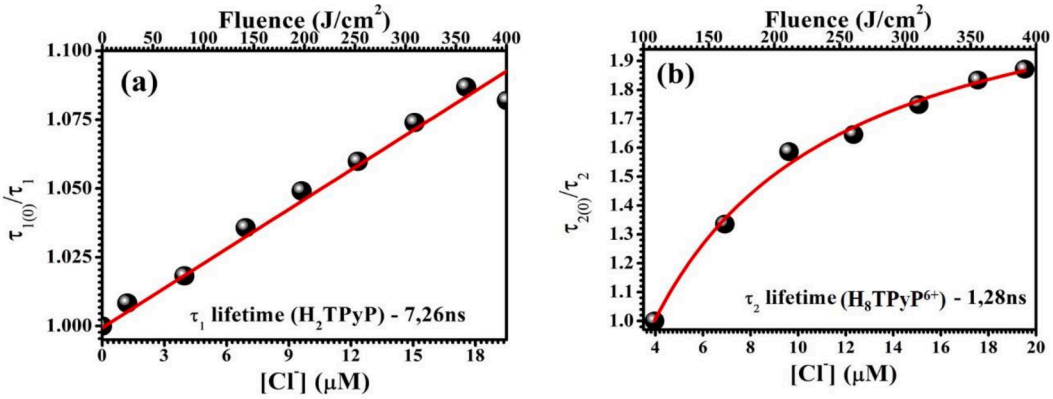

Fig. 3. Stern-Volmer plots for (a) $\frac{\tau_{1(0)}}{\tau_1}$ (H_2TPyP) and (b) $\frac{\tau_{2(0)}}{\tau_2}$ (H_8TPyP^{6+}). In both figures, black spheres represent SV values as a function of $[Cl^-]$ (in μM). The red solid curves are fittings using (a) Eq. (1) and (b) Eq. (2). The porphyrins are dissolved in $CHCl_3$.

$$\frac{\tau_{2(0)}}{\tau_2} = \frac{\{1 + \frac{\tau_{2(0)}}{\tau_{excip}} K([Cl^-] - [Cl_c^-])\}}{\{1 + K([Cl^-] - [Cl_c^-])\}}, \quad (2)$$

where $[Cl_c^-] = 0$, $\tau_{2(0)}$ is the unquenched lifetime, τ_2 is the quenched lifetime and τ_{excip} is the non-emissive exciplex lifetime. In our case, $[Cl_c^-] = 4.05$ μM is the critical concentration below which the lifetime associated with H_8TPyP^{6+} is not detectable, $\tau_{2(0)}$ (τ_2) is the unquenched (quenched) H_8TPyP^{6+} lifetime, and τ_{excip} is the H_8TPyP^{6+}/Cl^- non-emissive exciplex lifetime. After fitting, the parameters obtained from the H_8TPyP^{6+}'s SV plot are $K \cong 12.45 \times 10^4 M^{-1}$ and τ_{excip} 557 ± 45 ps. The fitting result shows that $K \approx 25.5\ K_{SV}$, which endorses the effectiveness of Cl^- interactions with H_8TPyP^{6+}.

3.4. ESA photo-induced modification of H_8TPyP^{6+}.

Next, we pay close attention to the evolution of the system for fluences from 400 to 1000 J/cm^2. Fig. 4a and b show representative B- and Q-band spectra for 0 J/cm^2, 400 J/cm^2, and 1000 J/cm^2 (Fig. S8 in SI shows the complete spectral set from 0 J/cm^2 to 1000 J/cm^2).

It is clear that both bands are losing their once well-structured spectral features. In one hand, the B-band spectra for delivered fluences above 400 J/cm^2 (Fig. 4a) clearly show that the H_2TPyP intensity pattern (decreasing with increasing fluence) no longer reflects an increase of the X-band's intensity (see Fig. S8a in SI). The inset in Fig. 4a shows that after reaching the threshold fluence (400 J/cm^2), the H_2TPyP B-band's intensity continuous to present a sigmoidal behavior with increasing fluence, while an abrupt decrease followed by a stationary behavior is observed for the X-band's intensity. The stationary behavior observed for the X-band indicates that both, the novel structure and the H_8TPyP^{6+} formations are happening at similar rates. On the other hand, the Q-band spectra at 1000 J/cm^2 in Fig. 4b clearly show that the vibronic progressions are modified as well. The behaviors presented by the B- and Q-bands are a strong indication that the original structures are undergoing structural changes.

It is known that protonated porphyrins are susceptible to undergo aggregation after favorable conditions are achieved (e.g. critical porphyrin concentrations or the presence of intermediator groups) [35,76,77]. Therefore, we hypothesize that there must be a fluence threshold associated with a critical H_8TPyP^{6+} concentration after which aggregate formation is greatly favored. In order to support this hypothesis, we performed ESA in previously protonated solutions (H_8TPyP^{6+} + $CHCl_3$), which were obtained via the addition of aliquots of HCl in our original solution (H_2TPyP + $CHCl_3$). The advantage of starting with such an acidic solution is that a previously fully protonated sample allows for precisely observing the evolution of the new spectral features after the critical fluence has been achieved, without the interference of H_2TPyP sub-products. Fig. S9 in SI shows the spectral evolution of the H_8TPyP^{6+} bands induced by pulsed irradiation. It is noticeable that a new band, which is red-shifted with relation to the H_8TPyP^{6+} original band, arises and gains intensity at the expense of decreasing the H_8TPyP^{6+} original band's intensity. This together with the existence of an isosbestic point strongly suggests the creation of a new ESA-driven species from the protonated H_2TPyP. Moreover, we also performed ESA-driven photo-protonation in *meso*-tetra(thienyl) porphyrin (H_2TThP), with similar 532 nm absorbance used for H_2TPyP. Our results show that the H_2TThP solution is completely protonated when excited with 1000 J/cm^2 of pulsed radiation (see Fig. S10 in the SI), being the protonation of the H_2TThP core the unique phenomenology observed [38]. Additionally, Muñoz et al., using ultraviolet continuum radiation (289 nm) also showed that the photo-protonated tetraphenyl porphyrin (H_4TPP^{2+}) is not converted in other species even after the complete protonation of the H_2TPP in solution [25]. Such results indicate that the protonated outlying pyridyl group is an important structural feature to form the new species. Indeed, the importance of protonated outlying groups also supports the possible aggregate formation, since in general charged outlying groups play important roles in the aggregation [35,76,77]. Supported by the experimental data we justify that the possible new species could likely be J-aggregates. The aggregation possibly takes place once the solution is rich in remnant Cl^- ions (subproducts of the porphyrin's protonation) interacting with the porphyrin ring and that likely work as intermediaries for the interactions between outlying pyridyl groups and the protonated cores of distinct H_8TPyP^{6+} [77].

4. Conclusion

In summary, we show that ESA applied to solutions of H_2TPyP dissolved in $CHCl_3$ is a reliable and efficient technique to controllably photo-induce $CHCl_3$ decomposition allowing for H_8TPyP^{6+} formation. Besides the use of ESA, the advantage of our method is that H_2TPyP behaves simultaneously as the mediator for PR and as the probe that facilitates the mapping of the mechanisms of such PR. We also demonstrate that after reaching a critical concentration of H_8TPyP^{6+}, ESA also controllably generates H_8TPyP^{6+} aggregates (possibly J-aggregates). Moreover, the multi-component character of the irradiated solution likely enables the occurrence of excited-state bi-molecular interactions, which we believe to be mediated by non-emissive exciplex, as suggested by the evolution of both H_2TPyP and H_8TPyP^{6+} PL lifetime. Finally, ESA-induced $CHCl_3$ decomposition provides an excellent opportunity to understand the role of the orbital's parity of the PR's reactant.

CRediT authorship contribution statement

J.M.S. Lopes: Data curation, Writing - original draft, Investigation,

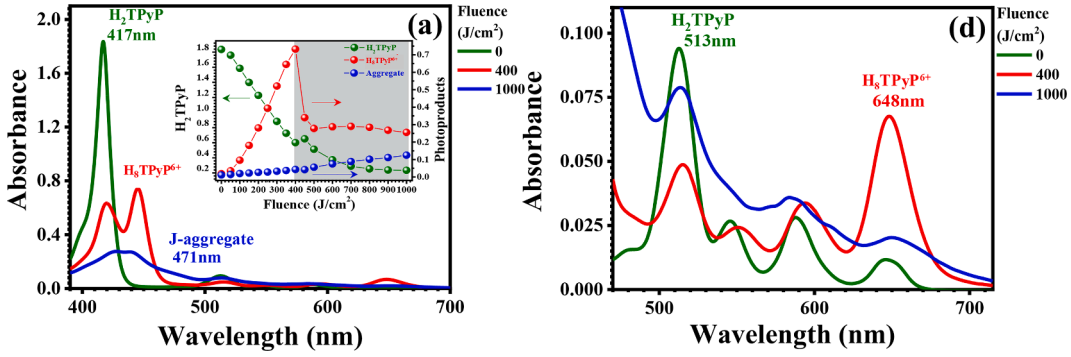

Fig. 4. (a) The absorbance spectra for solutions irradiated with 0 J/cm^2 (olive solid line), 400 J/cm^2 (red solid line) and 1000 J/cm^2 (blue solid line). (b)The zoom at the Q-band spectral region is presented. The inset in figure (a) compares the evolution of maxima value of the H_2TPyP B-band (olive spheres), the H_8TPyP^{6+} main band (red spheres) and, the new species bands (blue spheres). The porphyrins are dissolved in $CHCl_3$. In the inset, the area in gray delimits the fluence range for which the possible aggregate formation occurs.

Visualization, Formal Analysis, Methodology. **A.E.H. Machado:** Data Curation, Writing - original draft, Validation, Formal Analysis, Software. **A.A. Batista:** Writing - review & editing, Data curation, Formal Analysis, Project administration, Resources, Validation. **P.T. Araujo:** Data curation, Writing - original draft, Writing - review & editing, Visualization, Investigation, Fund Acquisition, Supervision, Project administration, Validation, Formal Analysis, Methodology. **N.M. Barbosa Neto:** Data curation, Writing - original draft, Writing - review & editing, Visualization, Investigation, Validation, Formal Analysis, Methodology, Supervision, Resources, Funding acquisition, Project administration.

Declaration of Competing Interest

The authors declare that they have no known competing financial interests or personal relationships that could have appeared to influence the work reported in this paper.

Acknowledgments

The authors are indebted to Brazilian agencies: CNPq under Grants No. [306147/2020-3], FAPESPA and CAPES under Grant No. [AUXPE 88881.159129/2017-01], FAPEMIG, National Institute for Science and Technology on Organic Electronic (INEO) and National Science Foundation (NSF – USA) under Grant No. [1848418] for the financial support. NMBN is especially grateful to Fulbright Foundation for the Visiting Professor Scholarship Award. The authors are grateful to professor Sanclayton Moreira, from the Graduate Program in Physics of the Federal University of Para for granting access to his experimental facilities.

Appendix A. Supplementary data

Supplementary data to this article can be found online at https://doi.org/10.1016/j.jphotochem.2021.113759.

References

[1] D. Krogmann, Discoveries in oxygenic photosynthesis (1727–2003): a perspective, Photosynth. Res. 80 (1-3) (2004) 15–58.
[2] P.J.M. Johnson, M.H. Farag, A. Halpin, T. Morizumi, V.I. Prokhorenko, J. Knoester, T.L.C. Jansen, O.P. Ernst, R.J.D. Miller, The primary photochemistry of vision occurs at the molecular speed limit, J. Phys. Chem. B 121 (16) (2017) 4040–4047.
[3] A. Wand, I. Gdor, J. Zhu, M. Sheves, S. Ruhman, Shedding new light on retinal protein photochemistry, Annu. Rev. Phys. Chem. 64 (1) (2013) 437–458.
[4] G.S. He, L.S. Tan, Q. Zheng, P.N. Prasad, Multiphoton absorbing materials: Molecular designs, characterizations, and applications, Chem. Rev. 108 (2008) 1245–1330.
[5] Q. Bellier, N.S. Makarov, P.-A. Bouit, S. Rigaut, K. Kamada, P. Feneyrou, G. Berginc, O. Maury, J.W. Perry, C. Andraud, Excited state absorption: a key phenomenon for the improvement of biphotonic based optical limiting at telecommunication wavelengths, Phys. Chem. Chem. Phys. 14 (44) (2012) 15299, https://doi.org/10.1039/c2cp40779e.
[6] Y. Kobayashi, K. Mutoh, J. Abe, Stepwise two-photon absorption processes utilizing photochromic reactions, J. Photochem. Photobiol. C Photochem. Rev. 34 (2018) 2–28.
[7] L. De Boni, A.A. Andrade, D.S. Corrêa, D.T. Balogh, S.C. Zilio, L. Misoguti, C. R. Mendonça, Nonlinear absorption spectrum in MEH-PPV/chloroform solution: a competition between two-photon and saturated absorption processes, J. Phys. Chem. B 108 (2004) 5221–5224.
[8] N.M. Barbosa Neto, L. De Boni, C.R. Mendonça, L. Misoguti, S.L. Queiroz, L. R. Dinelli, A.A. Batista, S.C. Zilio, Nonlinear absorption dynamics in tetrapyridyl metalloporphyrins, J. Phys. Chem. B 109 (36) (2005) 17340–17345.
[9] O. Laporte, W.F. Meggers, Some rules of spectral structure, J. Opt. Soc. Am. 11 (5) (1925) 459, https://doi.org/10.1364/JOSA.11.000459.
[10] M. Khurana, H.A. Collins, A. Karotki, H.L. Anderson, D.T. Cramb, B.C. Wilson, Quantitative in vitro demonstration of two-photon photodynamic therapy using Photofrin® and Visudyne®, Photochem. Photobiol. 83 (6) (2007) 1441–1448.
[11] R.L. Goyan, D. Cramb, Near-infrared two-photon excitation of protoporphyrin IX: photodynamics and photoproduct generation, Photochem. Photobiol. 72 (2000) 821–827.
[12] N.M.B. Neto, M.D.R. Silva, P.T. Araujo, R.N. Sampaio, Photoinduced self-assembled nanostructures and permanent polaron formation in regioregular poly (3-hexylthiophene), Adv. Mater. 30 (16) (2018) 1705052.
[13] S. Juodkazis, V. Mizeikis, K.K. Seet, M. Miwa, H. Misawa, Two-photon lithography of nanorods in SU-8 photoresist, Nanotechnology 16 (6) (2005) 846–849.
[14] H.B. Sun, S. Kawata, Two-photon photopolymerization and 3D lithographic microfabrication, Adv. Polym. Sci. 170 (2004) 169–273.
[15] D. Fu, T. Ye, T.E. Matthews, G. Yurtsever, W.S. Warren, Two-color, two-photon, and excited-state absorption microscopy, J. Biomed. Opt. 12 (5) (2007) 054004, https://doi.org/10.1117/1.2780173.
[16] H.C. Ishikawa-Ankerhold, R. Ankerhold, G.P.C. Drummen, Advanced fluorescence microscopy techniques-FRAP, FLIP, FLAP, FRET and FLIM, Molecules 17 (4) (2012) 4047–4132.
[17] M. Chang, J. Lee, N. Kleinhenz, B. Fu, E. Reichmanis, Photoinduced anisotropic supramolecular assembly and enhanced charge transport of poly(3-hexythiophene) thins films, Adv. Func. Mater 24 (2014) 4457–4465.
[18] I. Unger, G.P. Semeluk, The photolytic and photosensitized decomposition of chloroform, Can. J. Chem. 44 (12) (1966) 1427–1436.
[19] G.-J. Wang, R.-S. Zhu, H. Zhang, K.-L. Han, G.-Z. He, N.-Q. Lou, Photodissociation of chlorobenzene at 266 nm, Chem. Phys. Lett. 288 (2-4) (1998) 429–432.
[20] L.A. Peña, P.E. Hoggard, Photocatalysis of chloroform decomposition by hexachloroosmate(IV), Photochem. Photobiol. 86 (2) (2010) 467–470.
[21] L.A. Peña, P.E. Hoggard, Hexachlororhodate(III) and the photocatalytic decomposition of chloroform, J. Mol. Catal. A: Chem. 327 (1-2) (2010) 20–24.
[22] L.A. Peña, A.J. Seidl, L.R. Cohen, P.E. Hoggard, Ferrocene/ferrocenium ion as a catalyst for the photodecomposition of chloroform, Transit. Met. Chem. 34 (2) (2009) 135–141.
[23] R. Gilbert, M. Karabulut, P.E. Hoggard, Photocatalysis of chloroform degradation by μ-dichlorotetrachlorodipalladate(II), Inorganica Chim. Acta 363 (7) (2010) 1462–1468.
[24] C. Kormann, M.R. Hoffmann, D.W. Bahnemann, Photolysis of chloroform and other organic molecules in aqueous TiO2 suspensions, Environ. Sci. Technol. 25 (1991) 494–500.
[25] Z. Muñoz, A.S. Cohen, L.M. Nguyen, T.A. McIntosh, P.E. Hoggard, Photocatalysis by tetraphenylporphyrin of the decomposition of chloroform, Photochem. Photobiol. Sci. 7 (3) (2008) 337, https://doi.org/10.1039/b713270k.
[26] A.J. Seidl, L.R. Cohen, L.A. Peña, P.E. Hoggard, Chlorochromate ion as a catalyst for the photodegradation of chloroform by visible light, Photochem. Photobiol. Sci. 7 (11) (2008) 1373, https://doi.org/10.1039/b814585g.
[27] J.M.S. Lopes, K. Sharma, R.N. Sampaio, A.A. Batista, A.S. Ito, A.E.H. Machado, P. T. Araújo, N.M. Barbosa Neto, Novel insights on the vibronic transitions in free base meso-tetrapyridyl porphyrin, Spectrochim. Acta - Part A Mol Biomol. Spectrosc. 209 (2019) 274–279.
[28] D. Dolphin, The Porphyrins, Volume III, Phys. Chem., Part A, The Porphyrins 3 (1978) 640.
[29] N.M. Barbosa Neto, L. De Boni, J.J. Rodrigues Jr., L. Misoguti, C.R. Mendonça, L. R. Dinelli, A.A. Batista, S.C. Zilio, Dynamic saturable optical nonlinearities in free base porphyrins, J. Phorphyrins Phthalocyanines 7 (2003) 452–456.
[30] P.J. Gonçalves, L.D. Boni, N.M.B. Neto, J.J. Rodrigues, S.C. Zílio, I.E. Borissevitch, Effect of protonation on the photophysical properties of meso-tetra (sulfonatophenyl) porphyrin, Chem. Phys. Lett. 407 (1-3) (2005) 236–241.
[31] M. Kruk, A. Karotki, M. Drobizhev, V. Kuzmitsky, V. Gael, A. Rebane, Two-photon absorption of tetraphenylporphin free base, J. Lumin. 105 (1) (2003) 45–55.
[32] W.R. Dichtel, J.M. Serin, C. Edder, J.M.J. Fréchet, M. Matuszewski, L.-S. Tan, T. Y. Ohulchanskyy, P.N. Prasad, Singlet oxygen generation via two-photon excited FRET, J. Am. Chem. Soc. 126 (17) (2004) 5380–5381.
[33] E.B. Fleischer, α, β, γ, δ-Tetra-(4-pyridyl)-porphine and some of its metal complexes, Inorg. Chem. 1 (3) (1962) 493–495.
[34] M. J. Frisch, G. W. Trucks, H. B. Schlegel, G. E. Scuseria, M. A. Robb, J. R. Cheeseman, G. Scalmani, V. Barone, G. A. Petersson, H. Nakatsuji, X. Li, M. Caricato, A. V. Marenich, J. Bloino, B. G. Janesko, R. Gomperts, B. Mennucci, H. P. Hratchian, J. V. Ortiz, A. F. Izmaylov, J. L. Sonnenberg, D. Williams-Young, F. Ding, F. Lipparini, F. Egidi, J. Goings, B. Peng, A. Petrone, T. Henderson, D. Ranasinghe, V. G. Zakrzewski, J. Gao, N. Rega, G. Zheng, W. Liang, M. Hada, M. Ehara, K. Toyota, R. Fukuda, J. Hasegawa, M. Ishida, T. Nakajima, Y. Honda, O. Kitao, H. Nakai, T. Vreven, K. Throssell, J. Montgomery, J. A., J. E. Peralta, F. Ogliaro, M. J. Bearpark, J. J. Heyd, E. N. Brothers, K. N. Kudin, V. N. Staroverov, T. A. Keith, R. Kobayashi, J. Normand, K. Raghavachari, A. P. Rendell, J. C. Burant, S. S. Iyengar, J. Tomasi, M. Cossi, J. M. Millam, M. Klene, C. Adamo, R. Cammi, J. W. Ochterski, R. L. Martin, K. Morokuma, O. Farkas, J. B. Foresman and D. J. Fox, Gaussian 16, Revision C.01.
[35] N.C. Maiti, S. Mazumdar, N. Periasamy, J- and H- aggregates of porphyrin-surfacftant complexes: time-resolved fluorescence and other spectroscopic Studies, J. Phys. Chem. B 102 (1998) 1528–1538.
[36] S.E. Rodrigues, A.E.H. Machado, M. Berardi, A.S. Ito, L.M. Almeida, M.J. Santana, L.M. Liao, N.M. Barbosa Neto, P.J. Gonçalves, Investigation of protonation effects on the electronic and structural properties of halogenated sulfonated porphyrins, J. Mol. Struct. 1084 (2015) 284–293.
[37] G. De Luca, A. Romeo, L.M. Scolaro, Aggregation properties of hyperporphyrins with hydroxyphenyl substituents, J. Phys. Chem. B 110 (29) (2006) 14135–14141.
[38] I. Gupta, M. Ravikanth, Spectroscopic properties of meso-thienylporphyrins with different porphyrin cores, J. Photochem. Photobiol. A Chem. 177 (2-3) (2006) 156–163.
[39] A.B. Rudine, B.D. DelFatti, C.C. Wamser, Spectroscopy of protonated tetraphenylporphyrins with amino/carbomethoxy substituents: hyperporphyrin effects and evidence for a monoprotonated porphyrin, J. Org. Chem. 78 (12) (2013) 6040–6049.
[40] C. Wang, C.C. Wamser, Hyperporphyrin effects in the spectroscopy of protonated porphyrins with 4-aminophenyl and 4-pyridyl meso substituents, J. Phys. Chem. A 118 (20) (2014) 3605–3615.

[41] M. Zannotti, R. Giovannetti, B. Minofar, D. Řeha, L. Plačková, C.A. D'Amato, E. Rommozzi, H.V. Dudko, N. Kari, M. Minicucci, Aggregation and metal-complexation behaviour of THPP porphyrin in ethanol/water solutions as function of pH, Spectrochim. Acta - Part A Mol Biomol. Spectrosc. 193 (2018) 235–248.
[42] J.R. Weinkauf, S.W. Cooper, A. Schweiger, C.C. Wamser, Substituent and solvent effects on the hyperporphyrin spectra of diprotonated tetraphenylporphyrins, J. Phys. Chem. A 107 (18) (2003) 3486–3496.
[43] G. De Luca, A. Romeo, L.M. Scolaro, Role of counteranions in acid-induced aggregation of isomeric tetrapyridylporphyrins in organic solvents, J. Phys. Chem. B 109 (15) (2005) 7149–7158.
[44] M. Zawadzka, J. Wang, W.J. Blau, M.O. Senge, Laser induced protonation of free base porphyrin in chloroform results in the enhancement of positive nonlinear absorption due to conformational distortion, J. Porphyr. Phthalocyanines 17 (11) (2013) 1129–1133.
[45] M.V. Vijisha, S. Parambath, R. Jagadeesan, C. Arunkumar, K. Chandrasekharan, Nonlinear optical absorption and optical limiting studies of fluorinated pyridyl porphyrins in chlorobenzene: an insight into the photo-induced protonation effects, Dye. Pigment. 169 (2019) 29–35.
[46] Y. Fang, J. Zhu, Y. Cui, L. Zeng, M.L. Naitana, Y.i. Chang, N. Desbois, C.P. Gros, K. M. Kadish, Protonation and electrochemical properties of pyridyl- and sulfonatophenyl-substituted porphyrins in nonaqueous media, ChemElectroChem 4 (8) (2017) 1872–1884.
[47] J.M.S. Lopes, R.N. Sampaio, A.S. Ito, A.A. Batista, A.E.H. Machado, P.T. Araujo, N. M.B. Neto, Evolution of electronic and vibronic transitions in metal(II) meso-tetra (4-pyridyl)porphyrins, Spectrochim. Acta - Part A Mol Biomol. Spectrosc. 215 (2019) 327–333.
[48] W. Blau, H. Byrne, W.M. Dennis, J.M. Kelly, Reverse saturable absorption in tetraphenylporphyrins, Opt. Commun. 56 (1) (1985) 25–29.
[49] N.K.M. Naga srinivas, S. Venugopal rao, D.V.G.L.N. Rao, B.K. Kimball, M. Nakashima, B.S. Decristofano, D. Narayana rao, Wavelength dependent studies of nonlinear absorption in zinc meso-tetra(p-methoxyphenyl)tetrabenzoporphyrin (Znmp TBP) using Z-scan technique, J. Porphyr. Phthalocyanines 05 (07) (2001) 549–554.
[50] M. Drobizhev, N.S. Makarov, T. Hughes, A. Rebane, Resonance enhancement of two-photon absorption in fluorescent proteins, J. Phys. Chem. B 111 (50) (2007) 14051–14054.
[51] D. Narayana Rao, Excited state dynamics in porphyrins in relevance to third-order nonlinearity and optical limiting, Opt. Mater. (Amst) 21 (1-3) (2003) 45–49.
[52] P.P. Kiran, D.R. Reddy, A.K. Dharmadhikari, B.G. Maiya, G.R. Kumar, D.N. Rao, Contribution of two-photon and excited state absorption in 'axial-bonding' type hybrid porphyrin arrays under resonant electronic excitation, Chem. Phys. Lett. 418 (4-6) (2006) 442–447.
[53] D.N. Bowman, J.C. Asher, S.A. Fischer, C.J. Cramer, N. Govind, Excited-state absorption in tetrapyridyl porphyrins: comparing real-time and quadratic-response time-dependent density functional theory, Phys. Chem. Chem. Phys. 19 (40) (2017) 27452–27462.
[54] N.M. Barbosa Neto, S.L. Oliveira, L. Misoguti, C.R. Mendonça, P.J. Gonçalves, I. E. Borissevitch, L.R. Dinelli, L.L. Romualdo, A.A. Batista, S.C. Zilio, Singlet excited state absorption of porphyrin molecules for pico- and femtosecond optical limiting application, J. Appl. Phys. 99 (12) (2006) 123103, https://doi.org/10.1063/1.2204350.
[55] A. Marcelli, P. Foggi, L. Moroni, C. Gellini, P.R. Salvi, Excited-state absorption and ultrafast relaxation dynamics of porphyrin, diprotonated porphyrin, and tetraoxaporphyrin dication, J. Phys. Chem. A 112 (9) (2008) 1864–1872.
[56] R.N. Sampaio, W.R. Gomes, D.M.S. Araujo, A.E.H. Machado, R.A. Silva, A. Marletta, I.E. Borissevitch, A.S. Ito, L.R. Dinelli, A.A. Batista, S.C. Zílio, P. J. Gonçalves, N.M. Barbosa Neto, Investigation of ground- and excited-state photophysical properties outlying complexes, J. Phys. Chem. A 116 (2012) 18–26.
[57] J.S. Baskin, H.Z. Yu, A.H. Zewail, Ultrafast dynamics of porphyrins in the condensed phase: I. Free base tetraphenylporphyrin, J. Phys. Chem. A 106 (2002) 9837–9844.
[58] Y.-P. Wu, Y.-S. Won, Pyrolysis of chloromethanes, Combust. Flame 122 (3) (2000) 312–326.
[59] A.S. Rao, Comparison of rate equation models for nonlinear absorption, Optik (Stuttg) 158 (2018) 652–663.
[60] B. Valeur, M.N. Berberan-Santos, Molecular Fluorescence: Principles and Applications, second ed., Wiley-VCH Verlag & Co, Weinheim, 2012.
[61] J.R. Lakowicz, Principles of Fluorescence Spectroscopy, third ed., Springer, New York, 2006.
[62] T. Forster, The exciplex, in: M. Gordon, W.R. Ware, (eds.) Academic Press, New York, 1975.
[63] J.M.S. Lopes, S.G.C. Moreira, N.M. Barbosa Neto, Selective inner-filter on the fluorescence response of chlorophyll and pheophytin molecules extracted from Caesalpinia echinata leaves, J. Braz. Chem. Soc. 31 (2020) 162–169.
[64] A.S. Verkman, M.C. Sellers, A.C. Chao, T. Leung, R. Ketcham, Synthesis and characterization of improved chloride-sensitive fluorescent indicators for biological applications, Anal. Biochem. 178 (2) (1989) 355–361.
[65] A. Martin, R. Narayanaswamy, Studies on quenching of fluorescence of reagents in aqueous solution leading to an optical chloride-ion sensor, Sensors Actuators, B Chem. 39 (1-3) (1997) 330–333.
[66] C. Huber, K. Fähnrich, C. Krause, T. Werner, Synthesis and characterization of new chloride-sensitive indicator dyes based on dynamic fluorescence quenching, J. Photochem. Photobiol. A Chem. 128 (1-3) (1999) 111–120.
[67] H. Miyaji, P. Anzenbacher Jr, J.L. Sessler, E.R. Bleasdale, P.A. Gale, Anthracene-linked calix[4]pyrroles: fluorescent chemosensors for anions, Chem. Commun. (17) (1999) 1723–1724, https://doi.org/10.1039/a905054j.
[68] T. Werner, K. Fahnrich, C. Huber, O.S. Wolfbeis, Anion-Induced Fluorescence Quenching, 1999, 70, 585–589.
[69] S. Jayaraman, A.S. Verkman, Quenching mechanism of quinolinium-type chloride-sensitive fluorescent indicators, Biophys. Chem. 85 (1) (2000) 49–57.
[70] C.M.G. dos Santos, T. McCabe, T. Gunnlaugsson, Selective fluorescent sensing of chloride, Tetrahedron Lett. 48 (18) (2007) 3135–3139.
[71] Z. Zhang, D.S. Kim, C.-Y. Lin, H. Zhang, A.D. Lammer, V.M. Lynch, I. Popov, O.Š. Miljanić, E.V. Anslyn, J.L. Sessler, Expanded porphyrin-anion supramolecular assemblies: environmentally responsive sensors for organic solvents and anions, J. Am. Chem. Soc. 137 (24) (2015) 7769–7774.
[72] R.S. Davidson, A. Lewis, Formation of exciplexes between aromatic hydrocarbons and halogen anions, J. Chem. Soc., Chem. Commun. (8) (1973) 262, https://doi.org/10.1039/c39730000262.
[73] N.P. Illsley, A.S. Verkman, Membrane chloride transport measured using a chloride-sensitive fluorescent probe, Biochemistry 26 (5) (1987) 1215–1219.
[74] V.N. Grosso, C.A. Chesta, C.M. Previtali, Evidence for nonemissive exciplexes in the singlet quenching of polycyclic aromatic hydrocarbons by polychlorobenzenes in cyclohexane, J. Photochem. Photobiol. A Chem. 118 (3) (1998) 157–163.
[75] M.G. Kuzmin, Exciplex mechanism of the fluorescence quenching in polar media, 1993, 65, 1653–1658.
[76] P.J. Gonçalves, D.S. Correa, P.L. Franzen, L. De Boni, L.M. Almeida, C. R. Mendonça, I.E. Borissevitch, S.C. Zilio, Effect of interaction with micelles on the excited-state optical properties of zinc porphyrins and J-aggregates, Spectro chim. Act A 112 (2013) 309–317.
[77] Y. Arai, H. Segawa, Cl- complexation induced H- and J-Aggregates of meso-tetrakis-(4-sulfonatothienyl)porphyin diacid in aqueous solution, J. Phys. Chems. B 115 (2011) 773–7780.